sciendo

ARTICIAL SATELLITES, Vol. 59, No. 2 – 2024
DOI: 10.2478/arsa-2024-0005

DETERMINATION OF THE TOPOGRAPHY-BOUNDED ATMOSPHERIC GRAVITY CORRECTION FOR THE AREA OF POLAND

Marek TROJANOWICZ, Monika KASPRZAK, Karolina JAWORSKA

Institute of Geodesy and Geoinformatics, Wroclaw University of Environmental and Life Sciences, C. K. Norwida 25, 50–375 Wroclaw, Poland

e-mails: marek.trojanowicz@upwr.edu.pl, 111179@student.upwr.edu.pl, 111175@student.upwr.edu.pl

ABSTRACT. The standard recommended atmospheric gravity correction is based on the International Association of Geodesy (IAG) approach. This correction introduced into the results of gravimetric measurements reduces, in a simplified way, the influence of the actual atmospheric masses and the atmospheric masses contained inside a reference ellipsoid from the determined gravity anomalies or disturbances. Model of the actual atmosphere used in the IAG approach does not take into account topography as the lower boundary of the atmosphere, assuming that the atmosphere consists of spherical, constant density layers. In this study, we determined and analysed the components of atmospheric gravity correction for the area of Poland and its surroundings, considering topography as the lower limit of the atmosphere. In the calculations, we used algorithms typical for determining the topographic gravity reduction, assuming a model of atmospheric density based on the United States Standard Atmosphere 1976 model. The topography-bounded gravity atmospheric correction values determined were within the limits of 0.748–0.886 mGal and were different from standard, approximate atmospheric correction values in the range of 0.011 mGal for points at the sea level up to 0.105 mGal for points located at an altitude of approximately 2600 m.

Keywords: atmospheric correction, atmospheric density, gravity correction

1. INTRODUCTION

The masses of the currently used reference ellipsoids (GRS80 or WGS84), which are models of the Earth's gravity field, also include the masses of Earth's entire atmosphere (Moritz, 1980; NIMA Agency, 2000). This means that the values of normal gravity also include a component resulting from all masses of the atmosphere shifted inside the ellipsoid. The atmospheric component of the actual gravity at any point located on the terrain surface (assuming that above the analysed point, the atmosphere consists of spherical, constant density layers) contains only the atmospheric masses lying below this point (e.g. Torge, 1989). To take into account differences in the influence of atmospheric masses on normal and actual gravity, it is recommended to introduce a gravitational atmospheric correction (Moritz, 1980; Hinze et al., 2005). This correction is small, but significantly higher than the measurement accuracy of currently used gravimeters, and it is normally determined by the so-called International

Association of Geodesy (IAG) method based on the following approximate equation (Hinze et al., 2005):

$$\delta g_{\mathrm{atm}} = 0.874 - 9.9 \times 10^{-5} h + 3.56 \times 10^{-9} h^2 \quad (1)$$

where h is the height of the point in metres and the correction result is in milligals.

The correction (Eq. 1) added to the measured gravity increases its value by the influence of atmospheric masses contained within the reference ellipsoid and reduces it by the influence of a simplified model of the actual atmospheric masses. Eq. (1) was given by Wenzel (1985) based on the concept proposed by Ecker and Mittermayer (1969). This concept assumes that the atmospheric masses constitute spherical homogeneous layers extending from the surface of the sphere as the lower boundary. Atmospheric corrections to gravity and geoid, which take into account the topographic surface as the lower surface of the atmosphere on a global scale, were first estimated by Anderson et al. (1975) and Anderson (1976). This approach was later extensively studied in various contexts. Sjöberg (1993) estimated a gradient of influence of atmospheric masses on gravity at the level of 0.05 mGal/km. Sjöberg (1998, 1999) and Sjöberg and Nahavandchi (2000) investigated the atmospheric gravity effect in Stokes' formula, delivering formulas for the direct atmospheric gravity and geoid effects based on spherical harmonic representation of the topography. This approach was than improved by Nahavandchi (2004) by including local topography in the calculations. The effect of atmospheric masses for the Stokes' problem was also discussed by Tenzer et al. (2006). The authors determined the direct and secondary indirect atmospheric effects for the area of Canada. Novak and Grafarend (2005) analysed the effect of atmospheric masses on spaceborne observables of the geopotential gradient vector and gravity gradient tensor. The atmospheric effects on the gravity field quantities at a global scale were determined by Tenzer et al. (2009). The authors used the expressions for spectral analysis of a gravitational field. In turn, Mikuška et al. (2008) demonstrated in several examples the importance of topography for the determined atmospheric gravity corrections. A detailed analysis of the gravitational effect of the topography-bounded atmosphere in New Zealand was carried out by Tenzer et al. (2010). The authors used the calculation approach based on an analytical integration procedure described in detail by Mikuška et al. (2006). The values of the gravitational effect of the topography-bounded atmosphere that they determined varied from -0.009 mGal (offshore) up to 0.203 mGal for the highest peak. They also compared their results with the IAG approach and showed differences more than 0.1 mGal.

The main goal of this study is to conduct analyses analogous to Tenzer et al. (2010) for a different type of terrain and using a slightly different approach. In our analyses, the topography-bounded atmospheric gravity corrections were calculated using procedures known for topographic reduction of the gravity.

2. METHODOLOGY AND DATA

2.1. The Approach

The atmospheric correction (Eq. 1) is the difference of two components. The first is the normal gravity component defined by the atmospheric masses contained within the reference ellipsoid (the normal gravity component g^{NA}), which can be defined as (e.g. Sjöberg, 1993):

$$g^{NA} = \frac{GM_a}{r^2} \quad (2)$$

where G is Newton's gravitational constant, M_a is the mean mass of the Earth's atmosphere and r is the geocentric radius of the computation point.

The second component (spherical atmospheric component g^{SA}) is determined by the atmospheric masses constituting spherical, homogeneous layers extending from the surface of the reference sphere as the lower boundary, and it can be written as

$$g^{SA} = \frac{GM_{(r-R)}}{r^2} \tag{3}$$

where $M_{(r-R)}$ denotes the sum of the masses of homogeneous, spherical layers of the atmosphere located between the reference sphere of the radius R and the computation point.

Hence, in general, we will define Eq. (1) as

$$\delta g_{\mathrm{atm}} = g^{NA} - g^{SA} \tag{4}$$

If topography is adopted as the lower boundary of the atmosphere, the gravity effect of atmospheric masses (g^{ETA}) will be defined as (Figure 1)

$$g^{\mathrm{ETA}} = -\frac{\partial V^{\mathrm{ETA}}}{\partial r} \tag{5}$$

where

$$V^{\mathrm{ETA}} = G \iiint_{\Omega} \frac{\rho_A}{l} dV_{\Omega} \tag{6}$$

In Eq. (6), Ω is the volume of integration, ρ_A is the atmosphere density distribution function, l is the distance between the attracting masses and the attracted point and dV_{Ω} is the element of volume. The Ω volume covers the masses of the atmosphere from the surface of the topography to a height at least equal to the highest mountain peaks.

Alternatively, the g^{ETA} component can be determined from the difference (Mikuška et al., 2008)

$$g^{\mathrm{ETA}} = g^{SA} - g^{TA} \tag{7}$$

where g^{TA} is the topographic–atmospheric correction equal to the gravity of all Earth topography, assuming its density is equal to the density of the atmospheric masses (Figure 1):

$$g^{TA} = -\frac{\partial V^{TA}}{\partial r} \tag{8}$$

where

$$V^{TA} = G \iiint_{\Theta} \frac{\rho_A}{l} dV_{\Theta} \tag{9}$$

In Eq. (9), Θ represents the volume of all Earth topography.

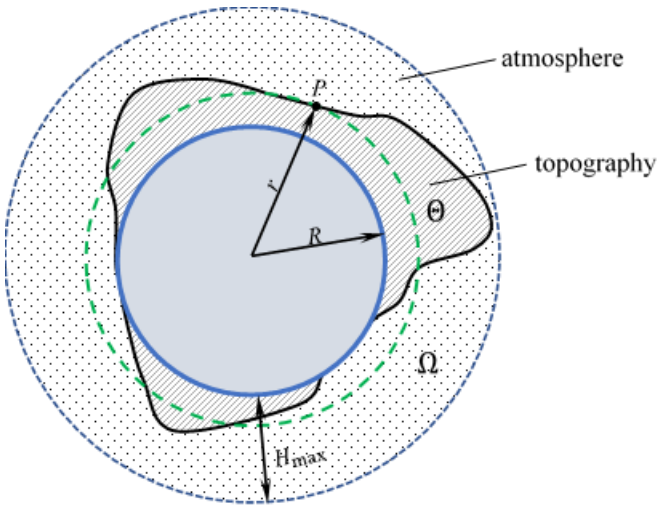

Figure 1. The Ω and Θ volumes adopted to determine the g^{ETA} component

Now, the topography-bounded atmospheric correction will be defined as

$$\delta g_{\mathrm{atm}}^{\mathrm{ETA}} = g^{NA} - g^{\mathrm{ETA}} \tag{10}$$

Let us note that taking into account the computational costs, determining the g^{ETA} component according to Eq. (7) is more advantageous than according to Eq. (5) due to the much smaller integration domain (in areas of seas and oceans, there is no topography, so they can be omitted). For this reason, we used it in further investigations.

The method of determination of Eq. (8) depends on the assumptions made regarding the coordinate system, available digital elevation model (DEM) and the atmospheric density distribution model. Assuming a spherical, geocentric coordinate system, DEM will be defined as a regular grid of spherical tesseroids.

By assigning each tesseroid a constant density ρ_A^i, the g^{TA} component can be determined based on

$$g^{TA} = \sum_{i=1}^{n} \delta g_i \tag{11}$$

In Eq. (11), n is the number of tesseroids used in the calculations and δg_i is the component of gravity determined based on a single tesseroid defined as (Heck and Seitz 2007)

$$\delta g_i = G\rho_A^i \int_{\lambda_1^i}^{\lambda_2^i} \int_{\varphi_1^i}^{\varphi_2^i} \int_{r_1^i}^{r_2^i} \frac{(r - r'\cos\psi) r'^2 \cos\varphi'}{l^3} dr' d\varphi' d\lambda' \tag{12}$$

where φ', λ' and r' are coordinates of the running integration point; λ_1^i, λ_2^i, φ_1^i, φ_2^i, r_1^i and r_2^i are the coordinates defining thesseroid i of DEM and ψ is the angle between the computation point (with coordinates φ, λ, r) and the running point:

$$\cos\psi = \sin\varphi \sin\varphi' + \cos\varphi \cos\varphi' \cos(\lambda' - \lambda) \tag{13}$$

Because there is no solution of the integral in Eq. (12) and the area of integration is very large and includes very distant masses, the δg_i components were determined using three

approximations. In the immediate vicinity of the calculation point (up to 5 km), tesseroids were replaced by rectangular prisms of the same mass, for which a closed solution of the appropriate integral is known (Nagy et al., 2000). For tesseroids located further away ($5 - 500$ km), we used the approximate solution of the integral in Eq. (12) in the form proposed by Heck and Seitz (2007). For further masses, tesseroids were replaced by point masses located in their centres.

Due to changes of atmospheric density in the vertical direction, determination of the g^{TA} component will also require vertically dividing individual DEM blocks into segments of appropriate height.

2.2. The Atmosphere Model

The United States Standard Atmosphere 1976 model (USSA76) was used to estimate the density of the atmosphere, ρ_A^i, needed to implement Eq. (12). Based on the tabular values included in model USSA76, an analytical model was determined using the least squares method in the form:

$$\rho_A(H) = \sum_{i=0}^{4} a_i H^i \tag{14}$$

where ρ_A is determined in $\mathrm{kg/m^3}$, H is the height in metres and a_i is a coefficient given in Table 1.

Table 1. The coefficients of model (Eq. 14) used in the calculations

Coefficient	Value
a_0	1.22499986
a_1	$-1.17606554 \times 10^{-4}$
a_2	$4.32023892 \times 10^{-9}$
a_3	$-7.34343434 \times 10^{-14}$
a_4	$5.18648018 \times 10^{-19}$

Based on the model (Eq. 14) and assuming $H = r - R$, the $M_{(r-R)}$ value can be written as the integral:

$$M_{(r-R)}(H) = 4\pi \int_0^H (R+H)^2 \rho_A(H) dH = 4\pi \int_0^H (R+H)^2 \left(\sum_{i=0}^{4} a_i H^i \right) dH \tag{15}$$

Its solution is given in the form:

$$M_{(r-R)}(H) = 4\pi \left(\sum_{i=0}^{4} s_i \right) \tag{16}$$

where:

$$s_0 = a_0 H \left(R^2 + RH + \tfrac{1}{3} H^2 \right);$$

$$s_1 = a_1 H^2 \left(\tfrac{1}{2} R^2 + \tfrac{2}{3} RH + \tfrac{1}{4} H^2 \right);$$

$$s_2 = a_2 H^3 \left(\frac{1}{3}R^2 + \frac{1}{2}RH + \frac{1}{5}H^2\right);$$

$$s_3 = a_3 H^4 \left(\frac{1}{4}R^2 + \frac{2}{5}RH + \frac{1}{6}H^2\right);$$

$$s_4 = a_4 H^5 \left(\frac{1}{5}R^2 + \frac{1}{3}RH + \frac{1}{7}H^2\right).$$

Eq. (16) allows determining the exact values of the g^{SA} component (Eq. 3), taking into account vertical atmospheric density changes in form of the model given by Eq. (14).

As delineated in the preceding section, owing to variations in atmospheric density along the vertical, the computation of the g^{TA} component according to Eqs (11) and (12), also requires the vertical partitioning of each individual DEM block into segments of suitable heights and constant density. To assess the vertical resolution of such segmentation, we will use the g^{SA} component, whose exact values can be determined. Let us note that the g^{SA} component (Eq. 3) can also be represented in an approximate form through the division of the atmosphere into m homogenous layers characterised by constant density and altitude. The $M_{(r-R)}$ value can, therefore, be expressed in the following form:

$$M_{(r-R)}(r) \cong \frac{4}{3}\pi \sum_{j=1}^{m-1} \rho_A^j (r_{j+1}^3 - r_j^3) \tag{17}$$

where $r_j = R + dh \times (j-1)$, $dh = \frac{r-R}{m}$ is the height of a single layer and ρ_A^j is the density of the atmosphere in the middle of the height of the layer j determined on the basis of Eq. (14).

The error in determining the g^{SA} component caused by using the approximate $M_{(r-R)}$ value defined by Eq. (17) instead of the exact value provided by Eq. (16) can be estimated by considering the difference:

$$\delta g^{SA} = g^{SA}_{\text{approx}} - g^{SA}_{\text{exact}} \tag{18}$$

where g^{SA}_{approx} and g^{SA}_{exact} represent the g^{SA} components determined using the $M_{(r-R)}$ values in their approximate form (Eq. 17) and exact form (Eq. 16), respectively.

To estimate the δg^{SA} errors for different dh, the g^{SA}_{approx} values were determined using Eqs (3) and (17) for one point situated at a height of 2,500 m (the highest point in the area of Poland) and for another point situated at a height of 8,500 m (the highest point on the Earth). Similarly, using Eqs. (3) and (16), the g^{SA}_{exact} values were determined for the same points. The determined δg^{SA} values are presented in Figure 2.

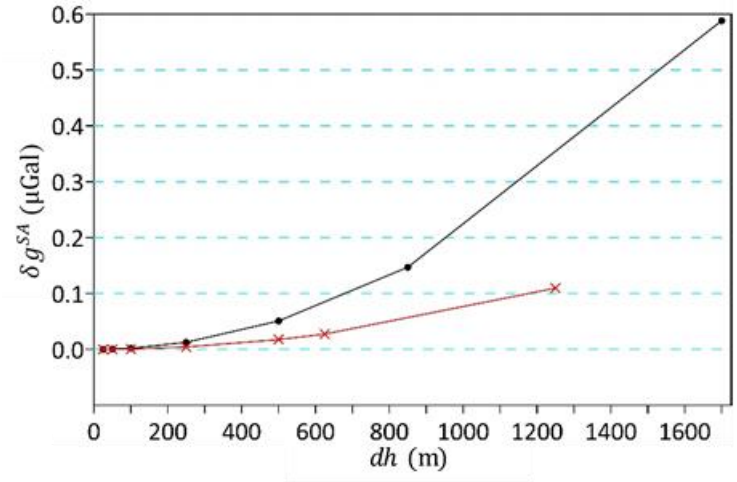

Figure 2. The δg^{SA} values for points with $H_p = 2{,}500$ m (red line) and $H_p = 8{,}500$ m (black line). The symbols in both charts indicate the dh values for which the calculations were performed.

Initially, it is noteworthy that the δg^{SA} error values are almost equal to 0 for $dh \leq 100$ m (in both analysed cases), whereas for $dh > 100$ m, they are noticeably larger for the point located at a higher elevation. This indicates that for points with heights lower than those examined, the δg^{SA} errors will not exceed the levels depicted in Figure 2. For instance, for points situated within the geographic boundaries of Poland (not exceeding 2,500 m in altitude), assuming $dh = 500$ m, the g^{SA}_{approx} component can be computed with the δg^{SA} errors not exceeding 0.02 μGal (as depicted by the red graph). Whereas, for locations not exceeding 8,500 m in elevation (i.e. points on the Earth's surface), the δg^{SA} errors may ascend to 0.05 μGal (as indicated by the black graph). Given that our calculations maintain an accuracy of approximately 1 μGal, such discrepancies remain within acceptable bounds.

The above discussed g^{SA} component errors also mirror those of the g^{TA} component, determined with the same vertical division of tesseroids constituting DEM. These errors will be equal if the topography consists of layers with constant heights (either 2,500 or 8,500 m, respectively). Consequently, the ascertained δg^{SA} errors for a height of 8,500 m can be considered the maximum errors in determining the g^{TA} component (for any point on the Earth's surface), resulting from the need to take into account changes in atmospheric density in the vertical direction by dividing tesseroids that constitute DEM into segments with constant of both atmospheric density and dh values. Considering the topography in the study area is generally lower overall, with the highest mountains situated at considerable distances, covering only a fraction of the Earth's surface, the error resulting from adopting $dh = 500$ m for the vertical tesseroids division will be substantially lower than the 0.05 μGal pointed above. Hence, $dh = 500$ m was selected to compute the g^{TA} component. Naturally, the g^{SA} component was determined in its exact version, based on Eqs (3) and (16).

2.3. The Study Area and DEM

The calculations were based on two DEMs: the SRTM v4.1 ($3'' \times 3''$ model) (Jarvis et al. 2008) and the ETOPO1 ($1' \times 1'$ model) (NOAA National Geophysical Data Center 2009). Based on these models, five sets of DEM were prepared and directly used in the calculations for various distances from the calculation point:

- $3'' \times 3''$ - model for calculations at a distance of up to approximately 10 km;
- $15'' \times 15''$- model for calculations at a distance of approximately $10 - 50$ km;

- $30'' \times 30''$- model for calculations at a distance of approximately $50 - 167$ km;
- $1' \times 1'$- model for calculations at a distance of approximately $167 - 500$ km;
- $6' \times 6'$- model for calculations carried out for topographic masses located further than 500 km.

The primary study area was located between parallels $48.4^{\circ} - 55.1^{\circ}$ and meridians $13.7^{\circ} - 24.5^{\circ}$ (Figure 3a). For this area, the calculations were performed for a regular grid of points with a resolution of $93'' \times 90''$. The area is mostly lowland. In the north, it covers a part of the Baltic Sea and in the south, it covers the Carpathian Mountains and the Sudetes (in the southwest). The highest region in the analysed area is the Tatra Mountains, with peaks reaching 2,499 m (Rysy) for the Polish part and 2,655 m (Gerlach) for the Slovak part of the Tatra Mountains. For part of the Tatra Mountains, marked in Figure 3a with a red rectangle, calculations were performed in a grid of points with a resolution of $12'' \times 9''$. This area is shown in Figure 3b.

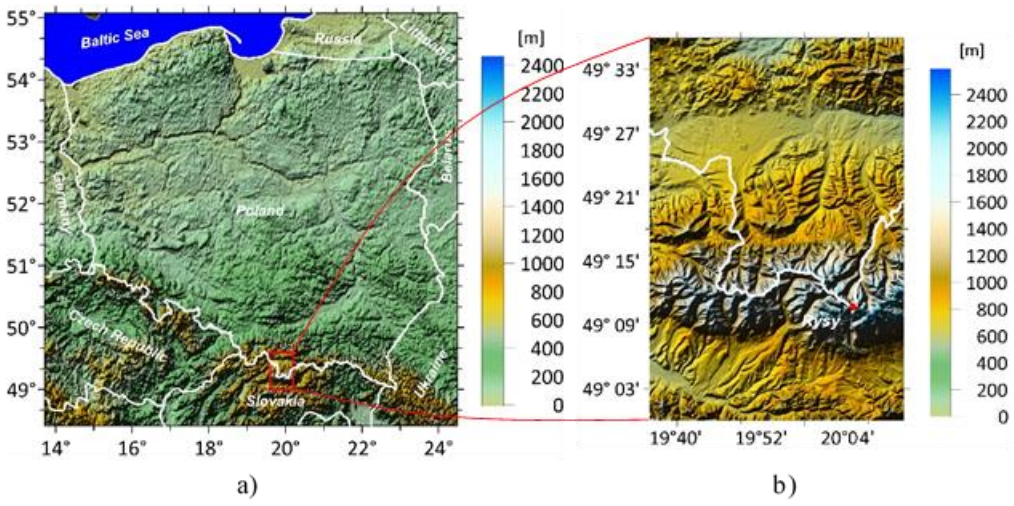

Figure 3. Relief maps of the study areas for a) the whole areas of elaboration and b) the Tatra mountains

3. RESULTS OF THE ANALYSES

First, the components g^{TA}, g^{SA} and g^{ETA} were determined. The statistics of these values are presented in Table 2.

Table 2. The statistics of the determined components of atmospheric gravity correction (mGal)

	min	**max**	**mean**	**st dev**
g^{TA}	0.012	0.108	0.033	0.019
g^{SA}	0.000	0.233	0.042	0.040
g^{ETA}	–0.012	0.125	0.009	0.021

All these components are strongly correlated with the height of the calculation point. These correlations are presented in Figure 4. Note that the g^{TA} component and, consequently, the g^{ETA} component depend not only on the height of the point, but also on the topography of its surroundings. This can be seen in the discrepancies in components for points of the same heights.

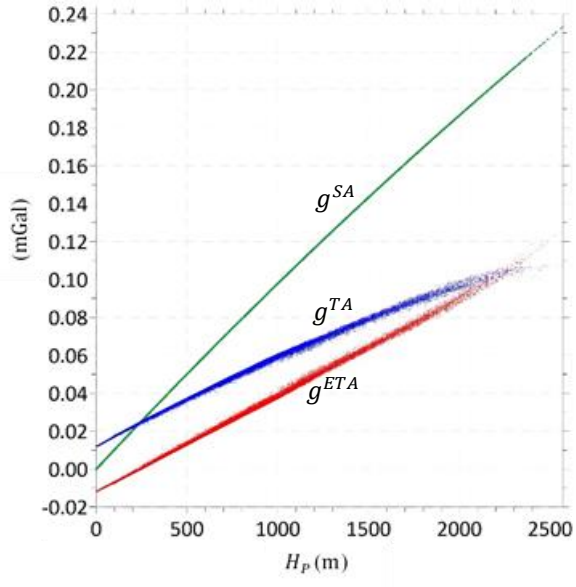

Figure 4. The correlation between the height of computation points and the values of g^{TA} – navy blue, g^{SA} – green and g^{ETA} – red

Component g^{ETA}, according to Eq. (7), is the difference of the two other components. The horizontal distribution of this component is shown in Figure 5.

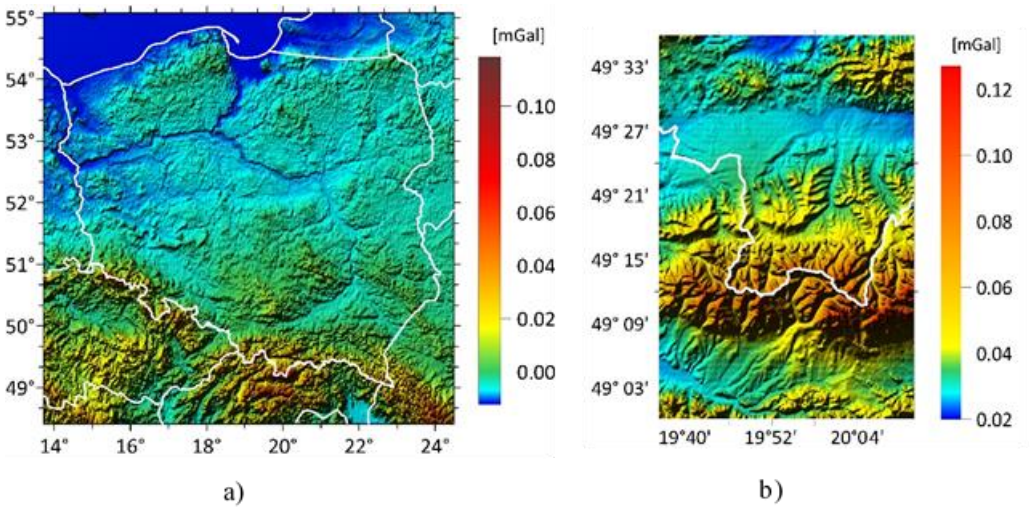

Figure 5. The g^{ETA} component: a) for the whole area of elaboration and b) for the Tatra mountains

The values of the g^{ETA} component are negative at points located on the sea surface (the lowest value was -0.012 mGal) and in low-altitude areas, up to approximately 220 m (Figure 4). For higher areas, the value is positive and reaches a value of 0.125 mGal for points with heights of 2600 m. As can be seen in Figure 5a and b, the values of this component reflect the topography of the area in detail.

Based on Eqs (1) and (10), the approximate (δg_{atm}) and topography-bounded $\left(\delta g_{\mathrm{atm}}^{\mathrm{ETA}}\right)$ atmospheric corrections were respectively determined. These values were compared to each other. Statistics of the corrections and the differences, as defined in the following equation:

$$\Delta\delta g_{\mathrm{atm}} = \delta g_{\mathrm{atm}} - \delta g_{\mathrm{atm}}^{\mathrm{ETA}} \tag{19}$$

are presented in Table 3.

Table 3. The statistics of the δg_{atm} and $\delta g_{\mathrm{atm}}^{\mathrm{ETA}}$ corrections as well as the differences, $\Delta\delta g_{\mathrm{atm}}$ (mGal)

	min	**max**	**max − min**	**mean**	**st dev**
$\boldsymbol{\delta g_{\mathrm{atm}}}$	0.643	0.875	0.232	0.833	0.039
$\boldsymbol{\delta g_{\mathrm{atm}}^{\mathrm{ETA}}}$	0.748	0.886	0.138	0.865	0.021
$\boldsymbol{\Delta\delta g_{\mathrm{atm}}}$	−0.105	−0.011	0.094	−0.032	0.018

Both corrections are strongly correlated with the heights of the analysed points. These correlations are presented in Figure 6.

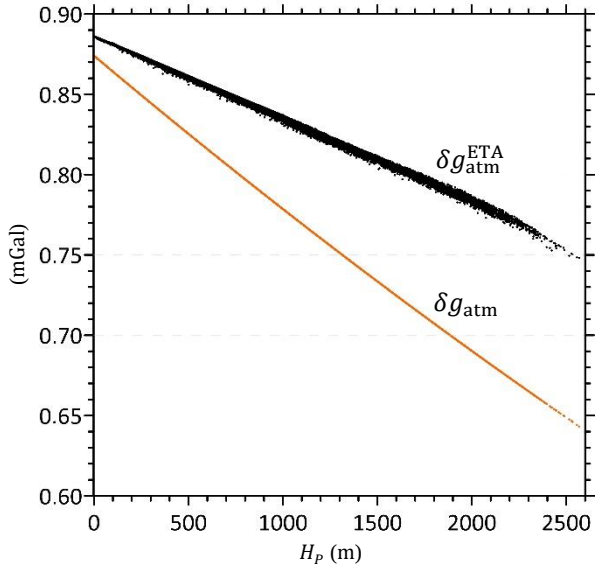

Figure 6. The correlations between the height of computation points and the corrections: $\delta g_{\mathrm{atm}}^{\mathrm{ETA}}$ – black and δg_{atm}– orange

As shown in Figure 6, the $\delta g_{atm}^{\mathrm{ETA}}$ correction (like the g^{ETA} component) takes slightly different values for points with the same height. This proves that its value is also influenced by relief of the point's surroundings. The most important differences, however, are between the approximate and topography-bounded corrections. For points located at the sea level, the differences are small and reach 0.011 mGal. They clearly increase with the height of the points, exceeding 0.1 mGal for points with heights of 2600 m. In relation to the total values of this correction, the differences shown can be considered as not very large. Please note, however, that the $\delta g_{\mathrm{atm}}^{\mathrm{ETA}}$ corrections vary only within a range of 0.138 mGal; hence, the differences at the level of 0.1 mGal should be assessed as significant. Let us also note that the results shown for the g^{ETA} component and the $\delta g_{\mathrm{atm}}^{\mathrm{ETA}}$ correction are consistent with those shown by Tenzer et al. (2010).

The horizontal distribution of the corrections $\delta g_{\mathrm{atm}}^{\mathrm{ETA}}$ and the $\Delta\delta g_{\mathrm{atm}}$ differences are presented in Figures 7 and 8, respectively.

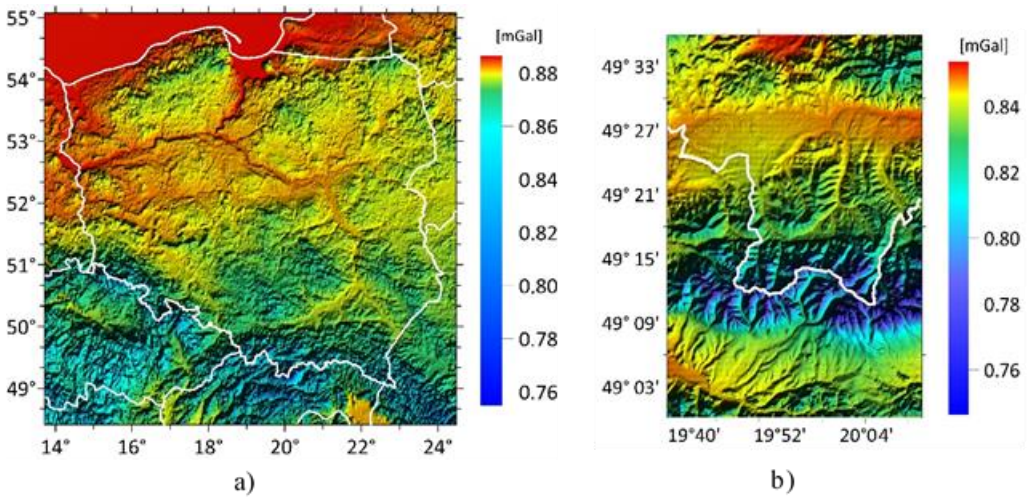

Figure 7. The $\delta g_{\mathrm{atm}}^{\mathrm{ETA}}$ corrections a) for the whole area of elaboration and b) for the Tatra mountains

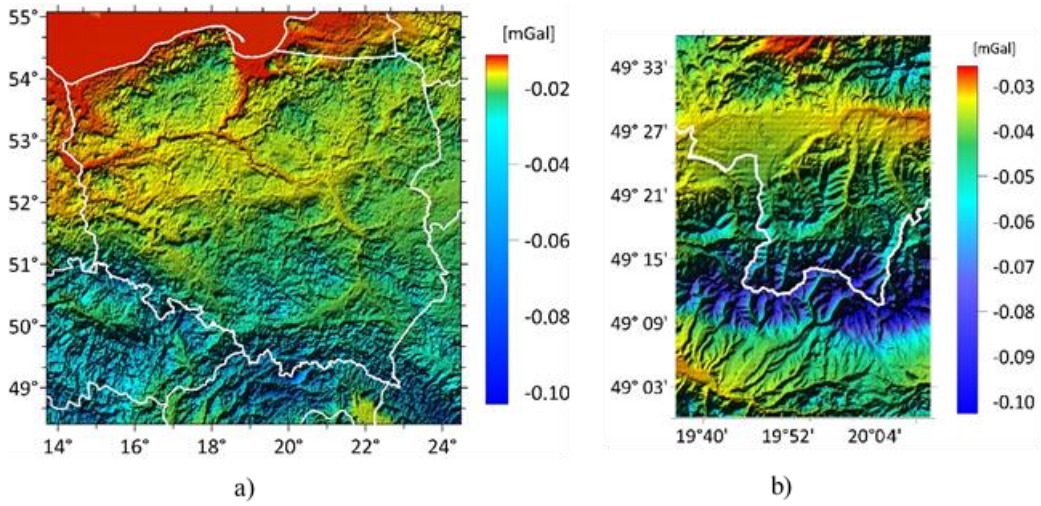

Figure 8. The differences $\Delta\delta g_{\mathrm{atm}}$ a) for the whole area of elaboration and b) for the Tatra mountains

4. CONCLUSIONS

The analyses performed showed that the values of the g^{ETA} component are negative (the lowest value was –0.012 mGal) at points located on the sea surface and for lowland areas, up to approximately 220 m (Figure 4). For higher located areas, it is positive and reaches a value of 0.125 mGal for points with heights of 2600 m. These values are strongly correlated with the heights of the points, but they also depend on the terrain relief around the computation point.

The topography-bounded gravity atmospheric correction ($\delta g_{\mathrm{atm}}^{\mathrm{ETA}}$) in the elaboration area ranges from 0.748 to 0.886 mGal. Like the g^{ETA} component, the values of this correction are strongly correlated with the heights of the points and also depend on the surrounding relief. Values of this correction are different from the commonly used approximate atmospheric correction, δg_{atm}, ranging from 0.011 mGal for points at the sea level up to 0.105 mGal for points located at an altitude of approximately 2600 m. These discrepancies are a trend and should be considered significant. The results obtained within this article confirm previous studies on the computation of the atmospheric gravity corrections (e.g. Tenzer et al., 2010).

REFERENCES

Anderson E. G. (1976) The effect of topography on solutions of Stokes's problem. *UNISURV Report S14, University of New South Wales, Kensington, Australia.*

Anderson E. G., Rizos C., Mather R. S. (1975) Atmospheric effects in physical geodesy. *UNISURV Report G23, University of New South Wales, Kensington, Australia.*

Ecker E., Mittermayer E. (1969) Gravity corrections for the influence of the atmosphere. *Bulletin of Theoretical and Applied Geophysics* 11, 70-80.

Heck B., Seitz K. (2007) A comparison of the tesseroid, prism and pointmass approaches for mass reductions in gravity field modelling. *Journal of Geodesy* 81(2),121–136.

Hinze W. J., Aiken C., Brozena J., Coakley B., Dater D., Flanagan G., Forsberg R., Hildenbrand T., Keller G. R., Kellogg J., Kucks R., Li X., Mainville A., Morin R., Pilkington M., Plouff D., Ravat D., Roman D., Urrutia-Fucugauchi J., Véronneau M., Webring M., Winester D. (2005) New standards for reducing gravity data: The North American gravity database. *Geophysics* 70, J25-J32.A.

Jarvis A., Reuter H. I., Nelson A., Guevara, E. (2008) Hole-filled SRTM for the globe Version 4. *The CGIAR-CSI SRTM 90m Database* (http://srtm.csi.cgiar.org).

Mikuška J., Marušiak I., Pašteka R., Karcol R., Beňo J. (2008) The effect of topography in calculating the atmospheric correction in gravimetry. *SEG Las Vegas Annual Meeting, SEG Technical Program Expanded Abstracts*, 784-788.

Mikuška J., Pašteka R., Marušiak I. (2006) Estimation of distant relief effect in gravimetry. *Geophysics* 71, J59-J69.

Moritz H. (1980) Geodetic Reference System 1980. *Journal of Geodesy,* 54, 395–405.

Nagy D., Papp G., Benedek J. (2000) The gravitational potential and its derivatives for the prism. *Journal of Geodesy*, 74, 552–560.

Nahavandchi H. (2004) A new strategy for the atmospheric gravity effect in gravimetric geoid determination. *Journal of Geodesy* 77, 823-828.

NIMA Agency (2000) TR8350.2, Third Edition, Amendment 1, January 3, 2000: e-report, accessed in 2004 to 2006.

NOAA National Geophysical Data Center (2009) ETOPO1 1 Arc-Minute Global Relief Model. NOAA National Centers for Environmental Information.

Novák P., Grafarend E. W. (2005) The effect of topographical and atmospheric masses on spaceborne gravimetric and gradiometric data. *Stud. Geophys. Geod.,* 50, 549-582.

Sjöberg L. E. (1993) Terrain effects in the atmospheric gravity and geoid correction. *Bulletin Géodesique,* 64, 178–184.

Sjöberg L. E. (1998) The atmospheric geoid and gravity corrections. *Bollettino di geodesia e scienze affini.,* N4.

Sjöberg L. E. (1999) The IAG approach to the atmospheric geoid correction in Stokes' formula and a new strategy. *Journal of Geodesy,* 73, 362-366.

Sjöberg L. E., Nahavandchi H. (2000) The atmospheric geoid effects in Stokes formula. *Geophysical Journal Internationa,l* 140, 95-100.

Tenzer R., Mikuška J., Marušiak I., Pašteka R., Karcol R., Vajda P., Sirguey P. (2010) Computation of the atmospheric gravity correction in New Zealand. *New Zealand Journal of Geology and Geophysics,* 53:4, 333-340.

Tenzer R., Novák P., Moore P., Vajda P. (2006) Atmospheric effects in the derivation of geoid-generated gravity anomalies. *Studia Geophysica and Geodaetica* 50, 583-593.

Tenzer R., Vajda P., Hamayun, (2009) Global atmospheric corrections to the gravity field quantities. *Contributions to Geophysics & Geodesy* 39(3), 221-236.

Torge W. (1989) Gravimetry. *Walter de Gruyter Publishing Co*.

Wenzel H. (1985) Hochauflösende Kugelfunktionsmodelle für das Gravitationspotential der Erde. *Wissenschaftliche arbeiten der Fachrichtung Vermessungswesen der Universität Hannover 137,* 1-155.

Received: *2024-04-05*

Reviewed: *2024-05-06 (R. Tenzer); 2024-06-12 (undisclosed name)*

Accepted: *2024-07-02*